PERGAMON

Deep-Sea Research I 49 (2002) 681–705

DEEP-SEA RESEARCH
PART I

www.elsevier.com/locate/dsr

Modification and pathways of Southern Ocean Deep Waters in the Scotia Sea

Alberto C. Naveira Garabato[a,*], Karen J. Heywood[a], David P. Stevens[b]

[a] *School of Environmental Sciences, University of East Anglia, Norwich NR4 7TJ, UK*
[b] *School of Mathematics, University of East Anglia, Norwich NR4 7TJ, UK*

Received 11 September 2000; received in revised form 11 June 2001; accepted 23 October 2001

Abstract

An unprecedented high-quality, quasi-synoptic hydrographic data set collected during the ALBATROSS cruise along the rim of the Scotia Sea is examined to describe the pathways of the deep water masses flowing through the region, and to quantify changes in their properties as they cross the sea. Owing to sparse sampling of the northern and southern boundaries of the basin, the modification and pathways of deep water masses in the Scotia Sea had remained poorly documented despite their global significance.

Weddell Sea Deep Water (WSDW) of two distinct types is observed spilling over the South Scotia Ridge to the west and east of the western edge of the Orkney Passage. The colder and fresher type in the west, recently ventilated in the northern Antarctic Peninsula, flows westward to Drake Passage along the southern margin of the Scotia Sea while mixing intensely with eastward-flowing Circumpolar Deep Water (CDW) of the antarctic circumpolar current (ACC). Although a small fraction of the other WSDW type also spreads westward to Drake Passage, the greater part escapes the Scotia Sea eastward through the Georgia Passage and flows into the Malvinas Chasm via a deep gap northeast of South Georgia. A more saline WSDW variety from the South Sandwich Trench may leak into the eastern Scotia Sea through Georgia Passage, but mainly flows around the Northeast Georgia Rise to the northern Georgia Basin.

In Drake Passage, the inflowing CDW displays a previously unreported bimodal property distribution, with CDW at the Subantarctic Front receiving a contribution of deep water from the subtropical Pacific. This bimodality is eroded away in the Scotia Sea by vigorous mixing with WSDW and CDW from the Weddell Gyre. The extent of ventilation follows a zonation that can be related to the CDW pathways and the frontal anatomy of the ACC. Between the Southern Boundary of the ACC and the Southern ACC Front, CDW cools by 0.15°C and freshens by 0.015 along isopycnals. The body of CDW in the region of the Polar Front splits after overflowing the North Scotia Ridge, with a fraction following the front south of the Falkland Plateau and another spilling over the plateau near 49.5°W. Its cooling (by 0.07°C) and freshening (by 0.008) in crossing the Scotia Sea is counteracted locally by NADW entraining southward near the Maurice Ewing Bank. CDW also overflows the North Scotia Ridge by following the Subantarctic Front through a passage just east of Burdwood Bank, and spills over the Falkland Plateau near 53°W with decreased potential temperature (by 0.03°C) and salinity (by 0.004). As a result of ventilation by Weddell Sea waters, the signature of the Southeast Pacific Deep Water (SPDW) fraction of CDW is largely erased in the Scotia Sea. A modified form of SPDW is detected escaping the sea via two distinct routes only: following the Southern ACC Front through Georgia Passage;

*Corresponding author. Fax: +44-1603-507719.
E-mail address: a.naveira-garabato@uea.ac.uk (A.C. Naveira Garabato).

PII: S0967-0637(01)00071-1

and skirting the eastern end of the Falkland Plateau after flowing through Shag Rocks Passage.

Keywords: Southern Ocean; Southwestern Atlantic; Scotia Sea; Circulation; Deep-water masses; Water mixing

1. Introduction

The deep water masses of the Southern Ocean are an essential component of the global thermohaline circulation. As postulated by Stommel and Arons (1960a,b), the oceanic heat balance is maintained through deep western boundary currents carrying cold, dense waters from the polar regions to lower latitudes, where they upwell (Rintoul, 1991; Gordon et al., 1992). Because the deep western boundary currents of the southern hemisphere are composed primarily of Southern Ocean waters (Mantyla and Reid, 1983), the properties and circulation of these waters are important factors in the climate system.

The Scotia Sea, a rather small region in the southwest Atlantic (Fig. 1), is thought to exert a disproportionately large influence on the composition of the deep western boundary currents of the southern hemisphere. There are two reasons for this. Firstly, the Scotia Sea provides a pathway for recently ventilated waters from the Weddell Sea to outflow into the deep western boundary current of the South Atlantic (Warren, 1981; Mantyla and Reid, 1983; Locarnini et al., 1993; Orsi et al., 1999). Secondly, it hosts an intense modification of the deep water masses advected into the region by the Antarctic Circumpolar Current (ACC) (Whitworth and Nowlin, 1987; Locarnini et al., 1993), which are the principal contributors to the boundary currents of the South Atlantic, South Pacific and Indian oceans (Mantyla and Reid, 1983; Orsi et al., 1999).

Weddell Sea Deep Water (WSDW) is the youngest and densest of the water masses escaping the Southern Ocean in a deep western boundary current (Orsi et al., 1999). From its primary source regions in the southwestern and western Weddell Sea (Fahrbach et al., 1995; Whitworth et al., 1998; Orsi et al., 1999), WSDW flows northward and eastward following the cyclonic Weddell Gyre (Orsi et al., 1993; Fahrbach et al., 1994). It may then escape the northern rim of the gyre through topographic clefts (Nowlin and Zenk, 1988; Locarnini et al., 1993), entering the Scotia Sea, or spread north over the South Sandwich Trench and the abyssal plains to the east (Orsi et al., 1993). Although subsequent northward flow is severely restricted by bathymetry and the plunging isopycnals of the eastward-flowing ACC (Orsi et al., 1999), some WSDW intrudes into the Argentine Basin through a deep breach in the Falkland Ridge (Whitworth et al., 1991) and becomes incorporated into the deep western boundary current of the South Atlantic (Arhan et al., 1999).

Amongst the water masses advected around the globe by the ACC, Circumpolar Deep Water (CDW) is the most voluminous. Its denser fraction (Lower CDW, LCDW) is characterised by a salinity maximum, which is derived from North Atlantic Deep Water (NADW) intruding into the ACC in the Atlantic sector (Reid et al., 1977; Whitworth and Nowlin, 1987). The lighter, older Upper CDW (UCDW) is marked by an oxygen minimum and nutrient maxima whose sources are in the Indian and Pacific oceans (Callahan, 1972). During its passage through the Scotia Sea, CDW is cooled and freshened to an extent that is unparallelled in the rest of the Southern Ocean (Locarnini et al., 1993). This observation has been attributed to interaction with waters from the Weddell Sea, though the details of the process remain unclear. Locarnini et al. (1993) pointed out that the juxtaposition of CDW and WSDW in the Scotia Sea makes the region particularly well suited for intense diapycnal mixing between the two water masses. Whitworth et al. (1994), however, emphasised the role of the Weddell–Scotia Confluence in ventilating CDW along isopycnals.

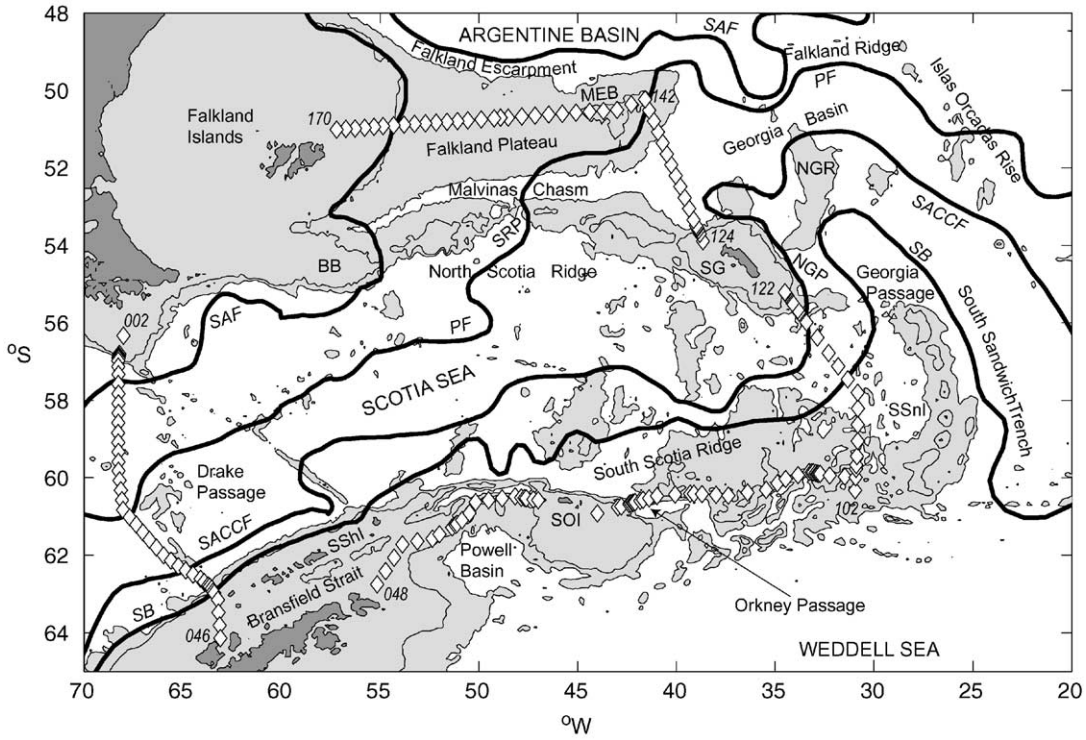

Fig. 1. Bathymetric configuration (isobaths 1500 and 3000 m) in the region of the Scotia Sea (Smith and Sandwell, 1997). ALBATROSS station positions (diamonds) and numbering are shown. Climatological trajectories of the ACC fronts, such as defined by Orsi et al. (1995), are superimposed (SAF = Subantarctic Front, PF = Polar Front, SACCF = Southern ACC Front, SB = Southern Boundary of the ACC). The path of the PF near the Maurice Ewing Bank and that of the SACCF in the western Georgia Basin have been modified after Trathan et al. (2000) and this study. The following topographic features are indicated by their initials: Burdwood Bank (BB), Maurice Ewing Bank (MEB), Northeast Georgia Passage (NGP), Northeast Georgia Rise (NGR), South Georgia (SG), South Orkney Islands (SOI), Shag Rocks Passage (SRP), South Shetland Islands (SShI), South Sandwich Islands (SSnI).

The Weddell–Scotia Confluence is a quasi-zonal band of eastward flow and weak stratification (Whitworth et al., 1994) extending from the northern end of the Antarctic Peninsula to 22°E (Orsi et al., 1993). It is bounded by the ACC to the north and is part of the northern limb of the Weddell Gyre. As well as CDW entrained from the ACC, it contains a high proportion of shelf water mixtures from the northwestern Weddell Sea and a cooler, fresher variety of LCDW that has circulated around the Weddell Gyre. This LCDW enters the Weddell Gyre through a broad discontinuity (25–32°E) in the Southwest Indian Ridge (Orsi et al., 1993) and is commonly referred to as Warm Deep Water (WDW).

An additional LCDW variety, resulting from interaction with the deep waters of the Ross Sea, is known to flow into the Scotia Sea with the ACC. Sievers and Nowlin (1984) named it Southeast Pacific Deep Water (SPDW) and identified a silicate maximum as its distinctive characteristic. Because it is formed downstream of the deep western boundary current of the South Pacific (Warren, 1981), SPDW was considered in the past to be of little global importance. This view has changed however since the detection of SPDW in the boundary current of the South Atlantic (Peterson and Whitworth, 1989; Arhan et al., 1999).

The spreading and modification of deep water masses in the Scotia Sea is subject to strong

bathymetric and dynamical constraints. The Scotia Sea is shallower than surrounding basins and, except at its western end (Drake Passage), is ringed by a system of ridges (Fig. 1). Discontinuities in these ridges are of extreme importance in determining flow patterns (Zenk, 1981; Nowlin and Zenk, 1988; Whitworth et al., 1991; Locarnini et al., 1993; Arhan et al., 1999) though, occasionally, they can be overshadowed by the relief of isopycnals. As isopycnic surfaces slope most abruptly at fronts, the frontal anatomy of the Scotia Sea is displayed schematically in Fig. 1.

In this paper, we make use of the ALBATROSS (Antarctic Large-scale Box Analysis and The Role Of the Scotia Sea) hydrographic data set to describe the pathways and quantify the changes in properties associated with each of the deep water masses crossing this globally important region. The data set is high-quality, quasi-synoptic and of high spatial resolution, and includes detailed information on the northern and southern boundaries of the sea. These, despite being key sites of water mass exchange with the mid-latitude South Atlantic and the Weddell Sea, have so far remained very sparsely sampled, and so the ALBATROSS data set makes a comprehensive description of the deep water mass modification and pathways in the Scotia Sea possible for the first time.

2. The ALBATROSS data set

The ALBATROSS data set was collected on board the RRS *James Clark Ross* during the period 15 March–22 April 1999 (Heywood and Stevens, 2000). It encompassed 165 hydrographic stations distributed along the periphery of the Scotia Sea (Fig. 1) and structured into five distinct hydrographic transects. The first of these involved a crossing of Drake Passage following the track of the World Ocean Circulation Experiment (WOCE) section S1/A21 with approximately doubled horizontal resolution and a southward extension across the Bransfield Strait. An unprecedented hydrographic line along the South Scotia Ridge, the poorly sampled southern boundary open to exchanges with the Weddell Sea, was then performed. This line ended at the intersection with the WOCE section A23, which was repeated northward as far as the island of South Georgia. The survey continued with a transect across the Georgia Basin between South Georgia and the Maurice Ewing Bank, and concluded with a section westward along the Falkland Plateau to the Falkland Islands. The latter transect had not been occupied previously and thereby provides the first sampling of the Falkland Plateau overflow water, which supplies the western boundary current of the South Atlantic. Typical station spacings of 27 km (Drake Passage), 23 km (South Scotia Ridge), 35 km (WOCE A23 repeat and Georgia Basin) and 38 km (Falkland Plateau) were used, with finer sampling in regions of steep bottom topography.

At each hydrographic station a Neil Brown Mark IIIc CTD and a FSI 24-bottle rosette multisampler were deployed to the ocean floor. All samples were analysed for salinity, dissolved oxygen and silicate. The data collection and analysis methods are described in the cruise report (Heywood and Stevens, 2000). The reported accuracies are 0.001°C in temperature and better than 0.002 in salinity, with precisions of 0.14% in oxygen and 1.5% in silicate.

Table 1
Definitions of the deep water masses of the Scotia Sea. Potential density ranges shown in the second column are from the literature (Reid et al., 1977 (RNP77); Sievers and Nowlin, 1984 (SN84); Arhan et al., 1999 (AHK99)). The equivalent neutral density classes used in this study are given in the third column

Water mass	Potential density (kg m^{-3})	Neutral density (kg m^{-3})
UCDW	$\sigma_0 > 27.35$, $\sigma_2 < 37.00$ (RNP77, SN84)	$27.55 < \gamma^n < 28.00$
LCDW/WDW	$\sigma_2 > 37.00$, $\sigma_4 < 46.04$ (SN84)	$28.00 < \gamma^n < 28.26$
SPDW	$45.98 < \sigma_4 < 46.04$ (AHK99)	$28.20 < \gamma^n < 28.26$
WSDW	$46.04 < \sigma_4 < 46.16$ (AHK99)	$28.26 < \gamma^n < 28.40$

3. The deep water masses of the Scotia Sea

Inspection of the thermohaline properties of the deep waters of the Scotia Sea allows us to track the presence of the five water types introduced in Section 1. As these waters encompass a large range of depths in the region, we will use the neutral density variable (γ^n) developed by Jackett and McDougall (1997) to define water mass boundaries (Table 1). Fig. 2e summarises these definitions schematically.

In Fig. 2, WSDW is characterised by a potential temperature (θ) in the range $-0.7<\theta<0.2^{\circ}$C and salinity (S) below 34.70. $\theta=-0.7^{\circ}$C was chosen by Carmack and Foster (1975) to differentiate between WSDW, which can overflow the South

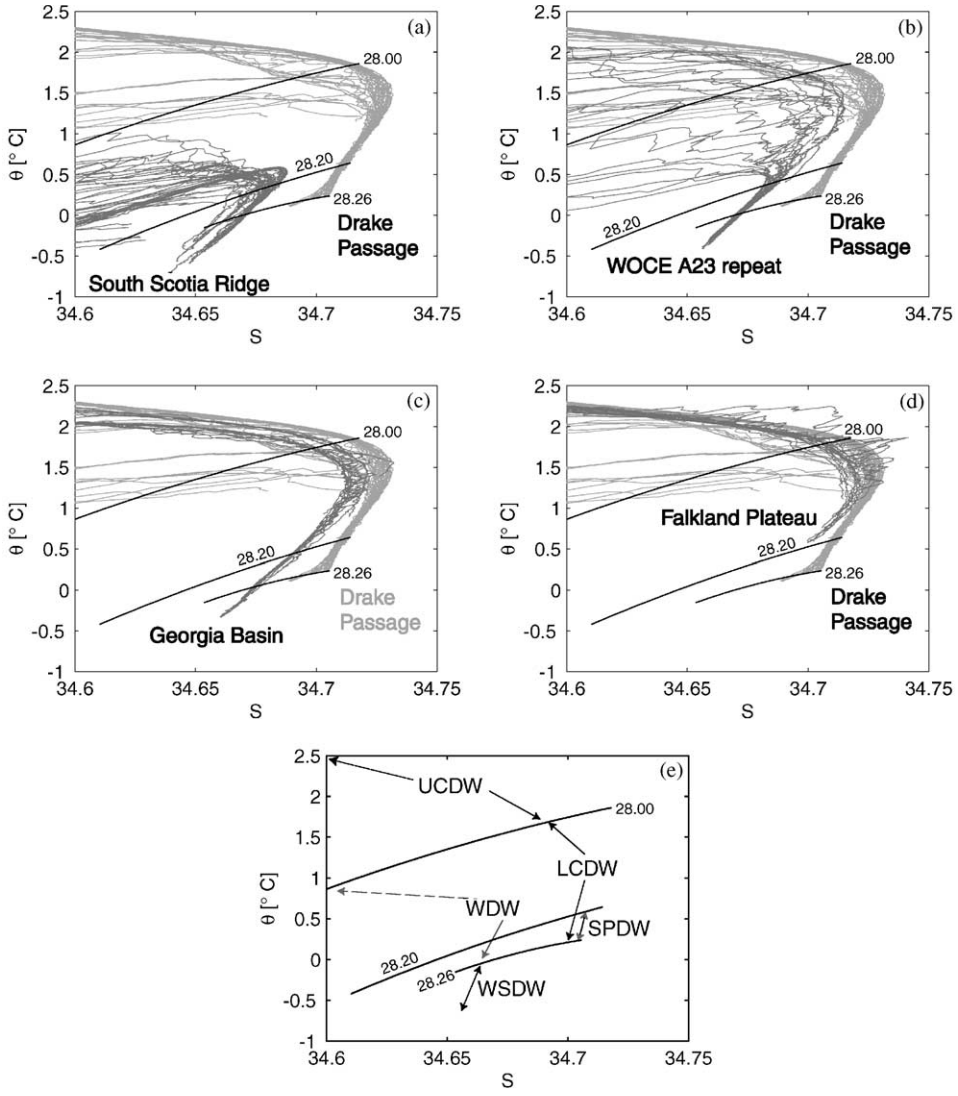

Fig. 2. Potential temperature–salinity curves for the deep waters sampled during ALBATROSS [(a) South Scotia Ridge, (b) WOCE A23 repeat, (c) western Georgia Basin, (d) Falkland Plateau]. The deep waters of Drake Passage are shown in all four panels for comparison. Solid lines represent neutral density contours at selected water mass boundaries. As neutral density is not only a function of temperature and salinity (but also of pressure, latitude and longitude) these contours are computed by fitting second order polynomials to the entire ALBATROSS data set. A schematic of water mass definitions is shown in (e).

Scotia Ridge, and the denser Weddell Sea Bottom Water, which cannot (cf. the coldest potential temperature in Fig. 2a). In the southwest Atlantic and Drake Passage, Reid et al. (1977) and Sievers and Nowlin (1984) identified a layer of enhanced stratification near $\theta = 0.2°C$ that signalled the transition between waters supplied by the ACC through Drake Passage and those of Weddell Sea origin. In Drake Passage, this layer coincides with the $\gamma^n = 28.26$[1] isopycnal, which is close to the upper bound of $\gamma^n = 28.27$ used by Orsi et al. (1999) in their definition of Antarctic Bottom Water. WSDW is detected in all but one of the five hydrographic transects (the exception is the Falkland Plateau section, Fig. 2d). Note that the WSDW in Drake Passage is markedly warmer and more saline than elsewhere in the study region, denoting intense diapycnal mixing with the overlying CDW.

LCDW in Drake Passage is characterised by salinity values generally above 34.70 and exceeding 34.73 at the mid-depth salinity maximum, with a potential temperature range of $0.2 < \theta < 1.9°C$. UCDW is warmer ($1.6°C < \theta < 3.2°C$) and fresher ($34.00 < S < 34.71$). The LCDW fraction colder than $\theta = 0.6°C$ and fresher than $S = 34.71$ is SPDW. Over the South Scotia Ridge, the density range of LCDW is occupied by WDW (Fig. 2a), distinguishable by its reduced potential temperature ($0.2°C < \theta < 0.6°C$) and salinity (at its mid-depth maximum, salinity remains below 34.69). WDW is also characterised by a mid-depth potential temperature maximum, for it is warmer than the overlying Antarctic Surface Water that fills the density range of UCDW south of the ACC (Orsi et al., 1995).

Both WDW and CDW from Drake Passage are observed in the WOCE A23 repeat section (Fig. 2b), where the detection of a group of waters with intermediate properties is indicative of upstream mixing between the two water masses. As a result, CDW in the ACC is now substantially cooler and fresher along isopycnals than that in Drake Passage, and the SPDW density range is mostly occupied by LCDW with WDW characteristics. These two features are also apparent in the Georgia Basin (Fig. 2c). The CDW of the Georgia Basin and, particularly, that of the Falkland Plateau, is closer in thermohaline properties to the CDW of Drake Passage. However, it remains slightly cooler and fresher than the latter, indicating that mixing with Weddell Sea waters in the Scotia Sea affects the entire width of the ACC. Also noticeable in Figs. 2c and d is the occurrence of a number of relatively warm and saline features with considerable fine structure in the proximity of the salinity maximum. These are attributable to entrainment of NADW, reported in the past at mid depths above the Falkland Escarpment (Peterson and Whitworth, 1989; Whitworth et al., 1991; Arhan et al., 1999).

4. Deep water mass modification and pathways

4.1. Weddell Sea Deep Water

4.1.1. The South Scotia Ridge overflow

The spatial distribution of WSDW over the South Scotia Ridge is shown in Fig. 3. Water denser than $\gamma^n = 28.26$ can be observed below about 1500 m, overflowing the ridge at the three deep passages east of the South Orkney Islands [located near 42°W (the Orkney Passage), 38°W (Bruce Passage) and 33°W (Discovery Passage)], and below 1300 m at the broad gap west of these islands [between 48 and 50°W (Philip Passage)]. In all four cases potential temperature, salinity and silicate reach a minimum at the sill of the passage, where a maximum in dissolved oxygen is also apparent.

Substantial geographical variability exists in the properties of WSDW spilling over the South Scotia Ridge. As illustrated in Fig. 4, the shallower WSDW west of the South Orkney Islands and in the 1350-m gap near 43°W is distinctively cooler (by about 0.1°C) and fresher (by about 0.01) [and also richer in oxygen (by about $5\,\mu mol\,kg^{-1}$) and poorer in silicate (by about $8\,\mu mol\,kg^{-1}$)] than that with the same neutral density in the deep passages to the east. This bimodal distribution of the properties and depth of WSDW along the transect suggests that WSDW overflowing

[1] The unit of density ($kg\,m^{-3}$) is omitted hereafter in the paper.

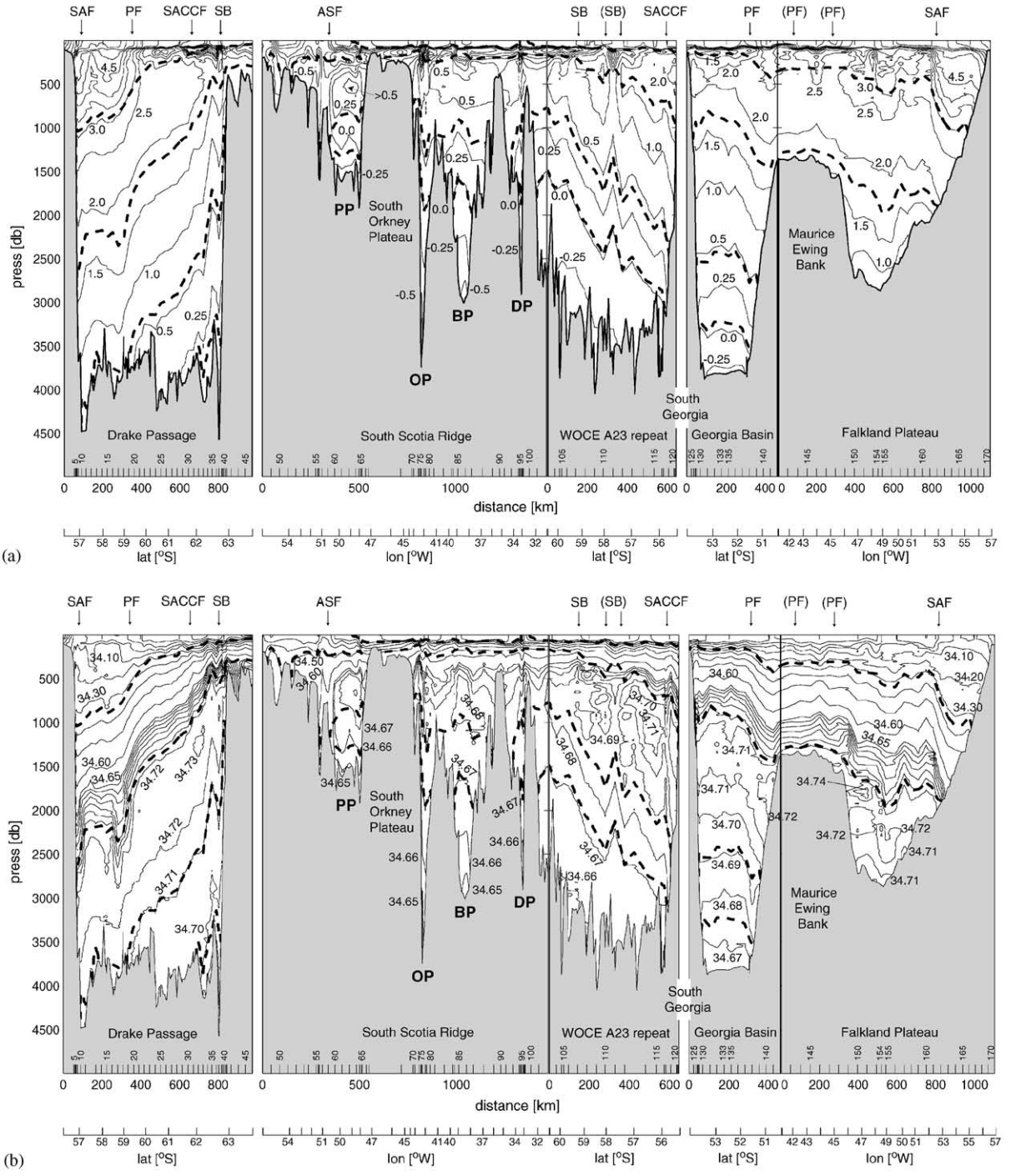

Fig. 3. Vertical distribution of (a) potential temperature (°C), (b) salinity, (c) dissolved oxygen (μmol kg^{-1}) and (d) dissolved silicate (μmol kg^{-1}) along the ALBATROSS cruise track. The locations of the ACC fronts (identified according to the definitions of Orsi et al. (1995)) are reported on the upper axis, with uncertain crossings in brackets. The position of the Antarctic Slope Front (ASF) as defined by Whitworth et al. (1998) is also indicated. The isopycnal boundaries defined in Section 3 are superimposed as thick dashed lines. The passages in the South Scotia Ridge are indicated by their initials (Philip Passage (PP), Orkney Passage (OP), Bruce Passage (BP), Discovery Passage (DP)). The spatial distribution of water masses is shown schematically in (e), along with relevant neutral density contours mentioned in the text.

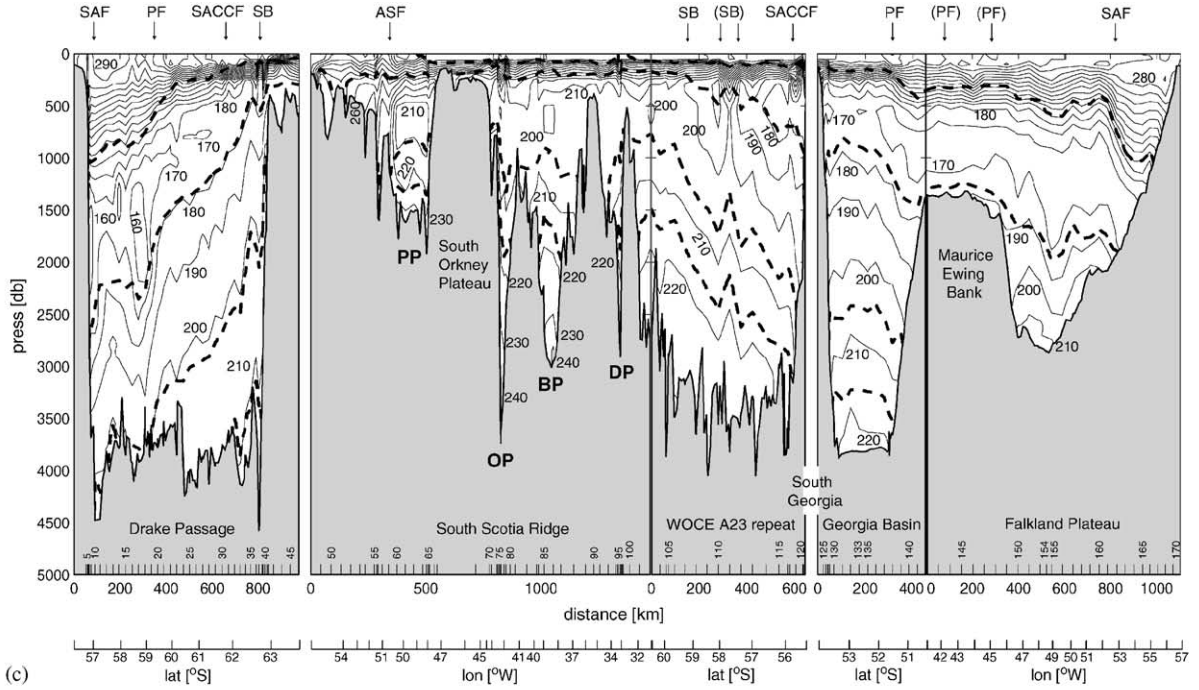

(c)

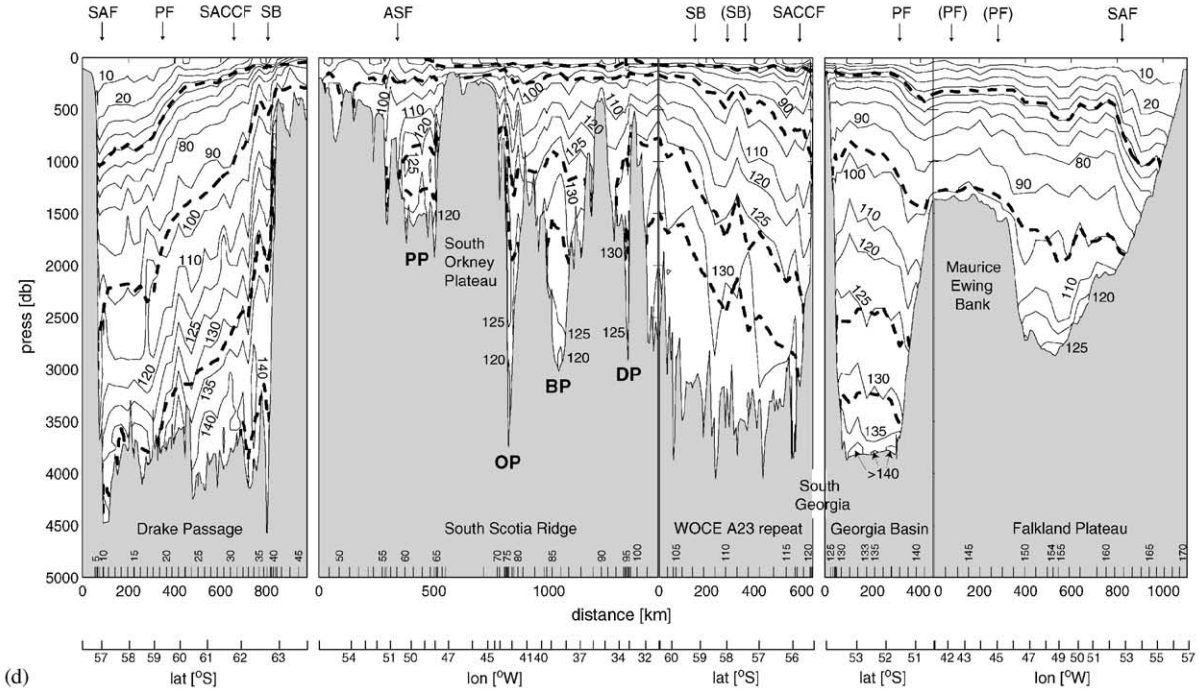

(d)

Fig. 3. (*Continued*)

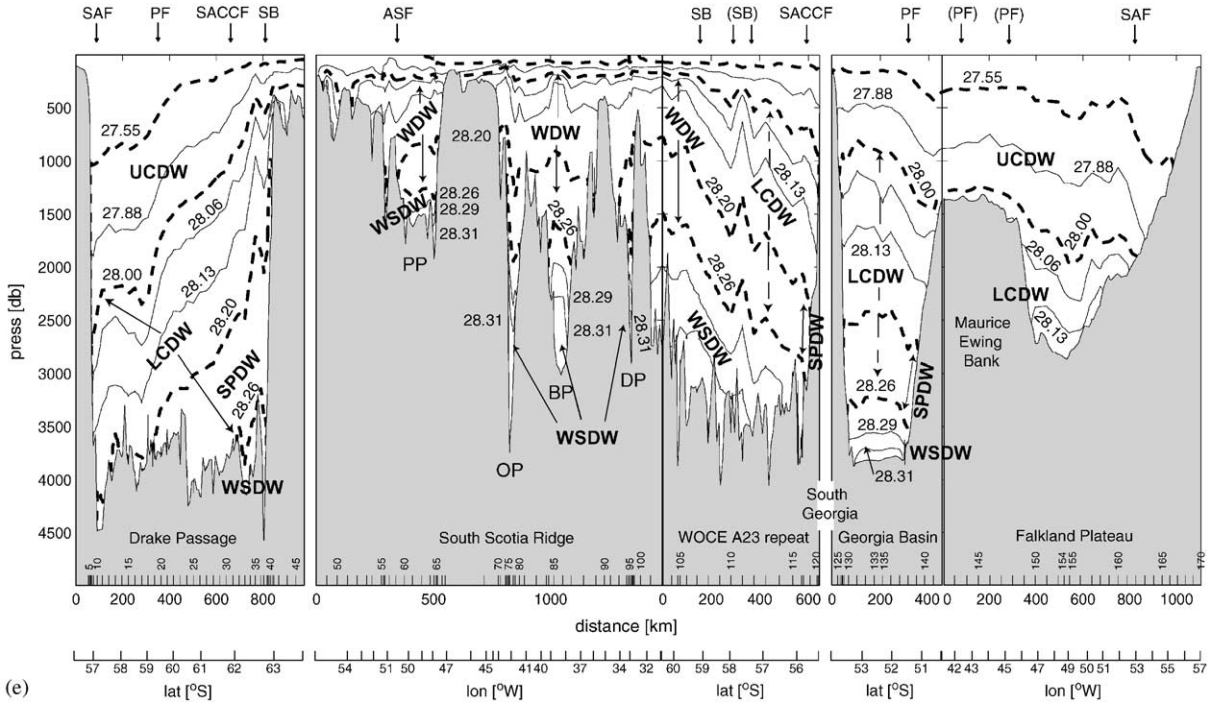

Fig. 3. (*Continued*)

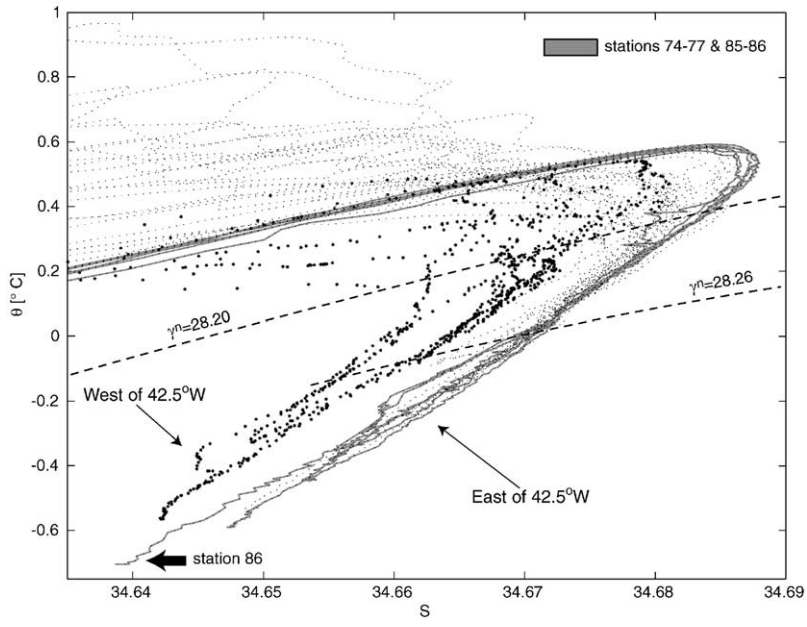

Fig. 4. Potential temperature–salinity plot for the deep waters above the South Scotia Ridge. Stations to the west (east) of 42.5°W are shown by large (small) dots. Stations 74–77 and 85–86 are shaded grey. Station 86 is indicated by the bold arrow. Dashed lines show selected neutral density contours.

the ridge west of 42.5°W (the western edge of the Orkney Passage) has a ventilation history different from that of WSDW further east.

Fahrbach et al. (1995) document the formation of WSDW off the northern Larsen Ice Shelf (approximately 500 km upstream of the South Scotia Ridge) from low salinity shelf waters spilling over the continental shelf edge and entraining WDW in the Weddell Gyre. They show that, immediately upstream of the Powell Basin (middle panel in their Fig. 2), the youngest fraction of the newly formed WSDW has barely initiated its descent down the continental slope and is shallower than 1600 m. Despite some sinking, part of this WSDW would be able to escape through Philip Passage (with a sill depth of 1900 m) if it followed the bathymetry, with some of the remaining WSDW skirting the southern flank of the South Orkney Plateau to flow through the 1350-m gap near 43°W. In contrast, the older, warmer and more saline WSDW that they observe further offshore and deeper in the water column would continue to flow east adjacent to the South Scotia Ridge until encountering one of the deeper passages to the east of the South Orkney Islands.

The detection of two distinct varieties of WSDW over the South Scotia Ridge and the patterns of circulation inferred here are consistent with the observations of Gordon et al. (2001) south of the ridge. They referred to the more recently ventilated WSDW type spreading into the Powell Basin and hugging the southern flank of the South Orkney Plateau as 'ventilated' WSDW, and suggested that 'ventilated' elements of WSDW and WSBW south of the South Scotia Ridge contribute (through diapycnal mixing) to the less oxygenated WSDW type. The same mixing process can be shown to occur as far downstream as ALBATROSS station 86 (Fig. 4), located at the centre of the Bruce Passage. There, the θ–S curve for $\theta < -0.4$°C bends gradually toward the lower salinity of the 'ventilated' WSDW as the sea floor is approached.

The fate of the 'ventilated' WSDW overflowing the South Scotia Ridge west of the Orkney Passage has not previously been ascertained. Having detected traces of the water mass over the northern flank of the ridge, Gordon et al. (2001) proposed that 'ventilated' WSDW follows a clockwise path along the isobaths of the South Orkney Trough (the deep channel to the north of the South Orkney Islands) to enter the interior of the Scotia Sea. They further pointed out that the shallowness of 'ventilated' WSDW and its privileged access to the Scotia Sea may confer the water mass with a dominant role in ventilating the Southwest Atlantic. These issues are addressed in the following by examining the characteristics of the WSDW leaving the Scotia Sea.

4.1.2. *The flow toward Drake Passage*

In Drake Passage, WSDW is confined to two contiguous troughs located between the SACCF at 62°S and the SB near 63°S (see caption of Fig. 1 for definitions of acronyms), as is apparent from the trajectory of the $\gamma^n = 28.26$ isopycnal in Fig. 3. Its volume is far smaller than that of the WSDW overflowing the South Scotia Ridge, with only the lightest fraction of the water mass being present in Drake Passage. As WSDW in Drake Passage is noticeably warmer (by about 0.1°C), more saline (by about 0.02), poorer in oxygen (by about 4 μmol kg^{-1}) and richer in silicate (by about 5 μmol kg^{-1}) along isopycnals than WSDW over the South Scotia Ridge, intense diapycnal mixing with an adjacent warmer, more saline water type (notably SPDW) must have occurred in the westward transit to Drake Passage. The Shackleton Fracture Zone near 57°W appears to be a key mixing site (Nowlin and Zenk, 1988). As a result of this mixing, little or no WSDW overflows Drake Passage into the Pacific Ocean (Orsi et al., 1999).

However, the properties of WSDW in Drake Passage are not entirely uniform (Fig. 5): the deepest water found at stations 38 and 39 (located above the continental slope, on the southern flank of the SB) is cooler (by 0.02°C), fresher (by about 0.003) and richer in oxygen (by 2 μmol kg^{-1}) than water with the same density at stations to the north. Although the density of the deepest water at station 38 ($\gamma^n = 28.259$) is just outside the range assigned to WSDW in Section 3, its spatially anomalous properties must apply equally to WSDW above the continental slope at a slightly greater depth. The signs of these anomalies are coincident with those of the properties of the

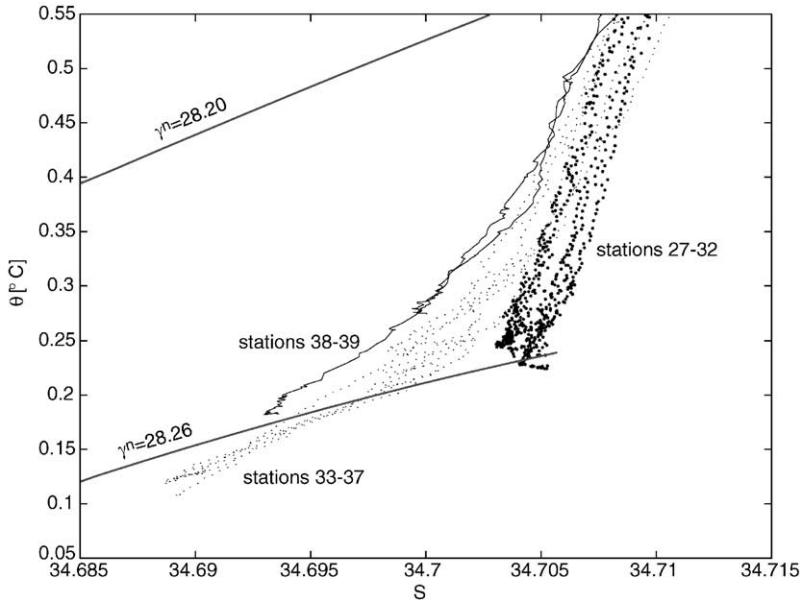

Fig. 5. Potential temperature–salinity plot for the deep waters in southern Drake Passage. Stations 27–32, north of the SACCF, are represented by large dots. Stations 33–37, between the SACCF and the SB, are shown by small dots. Stations 38–39, located south of the SB and above the continental slope, are depicted by a continuous trace. Selected neutral density contours are plotted as solid grey lines.

'ventilated' WSDW in relation to WSDW in the deep passages east of the South Orkney Islands. This suggests that the WSDW sequence detected above the continental slope in southern Drake Passage originates from WSDW spilling over the South Scotia Ridge west of the Orkney Passage and flowing westward above the northern flank of the ridge [where it was observed by Gordon et al. (2001)], with the WSDW in the troughs north of the continental slope being advected underneath the ACC from the Orkney Passage. The existence of two separate routes for WSDW to reach Drake Passage was first proposed by Nowlin and Zenk (1988) from a synthesis of hydrographic data and direct velocity measurements along the margin of the South Shetland Island Arc. As well as lending support to their hypothesis, the evidence presented here indicates that the two WSDW cores persist as separate entities as far as the sill of Drake Passage.

4.1.3. WSDW in the eastern Scotia Sea

In the WOCE A23 repeat section, a far larger volume of WSDW is observed than in Drake Passage (Fig. 3). WSDW spans the entire length of the transect south of the SACCF near South Georgia. Thermohaline variability in the WSDW density range is small and comparable to the accuracy of the measurements (Fig. 6). No WSDW of the 'ventilated' variety is detected in the section, and so no sign of the eastward-flowing 'ventilated' WSDW core proposed by Gordon et al. (2001) north of the South Orkney Islands is found. WSDW in the eastern Scotia Sea is predominantly supplied by flow through and east of the Orkney Passage. Although our data do not rule out the existence of an eastward 'ventilated' WSDW flow further west, we favour the view that this WSDW type is principally exported toward Drake Passage over the northern flank of the ridge. Subject to the vigorous mixing regime of Drake Passage, that 'ventilated' WSDW will probably be entrained into the CDW layer, and only then may return eastward with the ACC.

In addition to the South Scotia Ridge overflow, a new (though minor) WSDW contribution to the eastern Scotia Sea can be identified. Close inspection of the grey curves in Fig. 6 reveals an

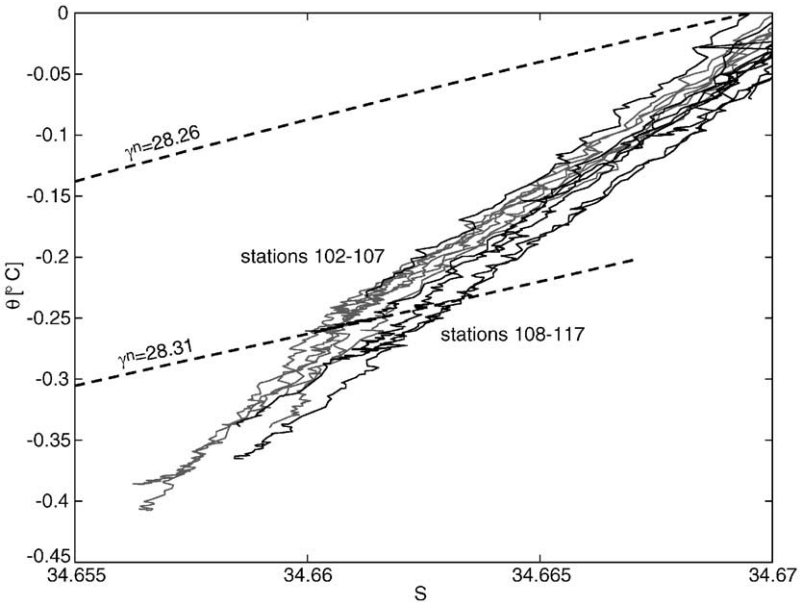

Fig. 6. Potential temperature–salinity plot for the deep waters in the WOCE A23 repeat section. Stations 102–107, south of the SB, are plotted in grey. Stations 108–117, between the SB and the SACCF, are shown in black. Dashed lines indicate selected neutral density contours.

inflection of the θ–S relationship south of the SB (stations 102–107), with θ–S curves bending toward a higher salinity at densities in excess of $\gamma^n = 28.31$. A likely origin of this feature is WSDW escaping the Weddell Sea along the South Sandwich Trench, which is more saline than that spilling over the South Scotia Ridge during ALBATROSS and several other cruises (Arhan et al., 1999; Gordon et al., 2001; Meredith et al., 2001). An eastern source is also suggested by the southward deepening trend of isopycnals in the vicinity of $\gamma^n = 28.31$ south of the SB, implying weak westward flow relative to the bottom.

With the available data, we cannot identify beyond doubt the site(s) at which the South Sandwich Trench WSDW has entered the Scotia Sea. The pronounced shallowing of isopycnals over the South Sandwich Island Arc [Orsi et al. (1999, Fig. 10)] indicates that multiple leakages of WSDW from the South Sandwich Trench into the Scotia Sea may occur through the various deep gaps between the islands [with a maximum sill depth of 2300 m (Smith and Sandwell, 1997)]. However, two observations suggest that the Georgia Passage, at the northern end of the island arc, may be the prime source of the saline WSDW end member: (1) the density of the θ–S inflection coincides almost exactly with that at the bottom of the Georgia Passage [$\sigma_4 = 46.09$ (Arhan et al., 1999)]; and (2) the discontinuity is confined to south of the SB, which also crosses the passage (Fig. 1). Thus, the natural meridional varibility in the northern limb of the Weddell Gyre can conceivably elicit an occasional flow through the Georgia Passage into the Scotia Sea of WSDW with a maximum density greater than the time-averaged density at the bottom of the passage. Below this density ($\gamma^n = 28.31$), the inflowing WSDW could contain a higher proportion of the saline South Sandwich Trench variety. Meredith et al. (2001) showed that the θ–S slope discontinuity is not a permanent feature of the WSDW in the eastern Scotia Sea, and elaborated on possible mechanisms for its intermittency.

4.1.4. The entry to the western Georgia Basin

Climatological maps of bottom potential temperature such as that of Locarnini et al. (1993,

Fig. 2) indicate that WSDW within the Scotia Sea does not extend as far north as the North Scotia Ridge, and that it can only reach the Georgia Basin via the Georgia Passage. They also show that WSDW escaping the Weddell Sea via the South Sandwich Trench is able to spread into the Georgia Basin. Further, they suggest that the entry of WSDW to the western Georgia Basin can occur via two distinct routes: by flowing through the Northeast Georgia Passage (the saddle between South Georgia and the Northeast Georgia Rise, see Fig. 1), or by circumnavigating the Northeast Georgia Rise.

The existence of these two routes is reflected in the θ–S relationship of the WSDW at the entry to the Malvinas Chasm (Fig. 7). θ–S curves across the section display an inflection (toward higher salinity for increasing depth) at a density of $\gamma^n = 28.29$, which is coincident with the density at the sill of the Northeast Georgia Passage [$\sigma_4 = 46.07$ (Arhan et al., 1999)]. The jump in salinity is suggestive of WSDW below that isopycnal (which must have flowed around the Northeast Georgia Rise) containing a comparatively higher proportion of the high-salinity variety from the South Sandwich Trench, with the WSDW layer above receiving a greater contribution of the fresher variety from the eastern Scotia Sea. The latter, less dense WSDW type would follow the SACCF from the Scotia Sea through the Northeast Georgia Passage (Fig. 1), as proposed by Arhan et al. (1999) and Orsi et al. (1999).

This view is consistent with the observations of Arhan et al. (1999) at 35°W in the western Georgia Basin. They showed (their Fig. 8b and c) that the entire WSDW layer in the vicinity of the Northeast Georgia Passage is markedly fresher along isopycnals than that filling the northern Georgia Basin, which indicates that the former is supplied from the eastern Scotia Sea and the latter from the South Sandwich Trench. Our data extend their picture by showing that a fraction ($\gamma^n > 28.29$) of the WSDW in the northern Georgia Basin can spread southwestward by underriding the less dense WSDW inflowing via the Northeast Georgia Passage. At the entry of the Malvinas Chasm, the salinity difference between the two WSDW types has been attenuated by diapycnal mixing, but a dominance of the fresher Scotia Sea variety is apparent by reference to Arhan et al. (1999, their

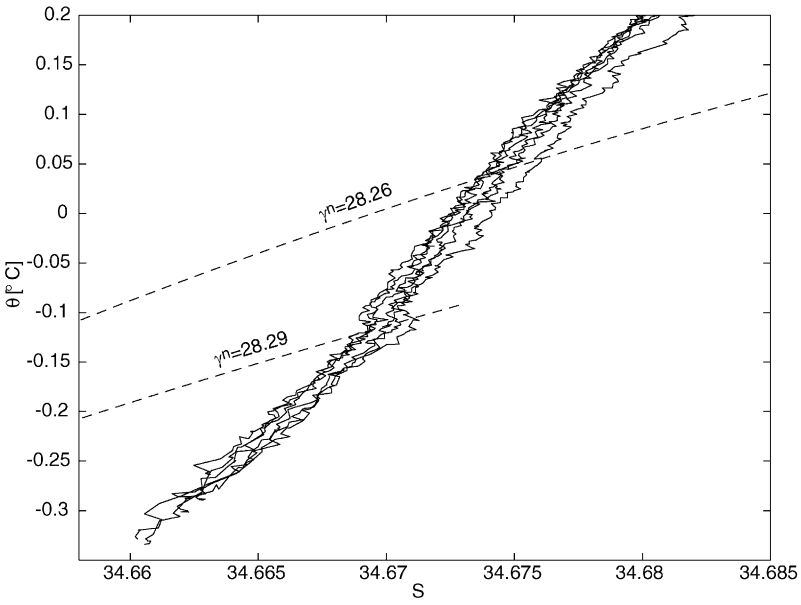

Fig. 7. Potential temperature–salinity plot for the deep waters in the western Georgia Basin. Selected neutral density contours are shown as dashed lines.

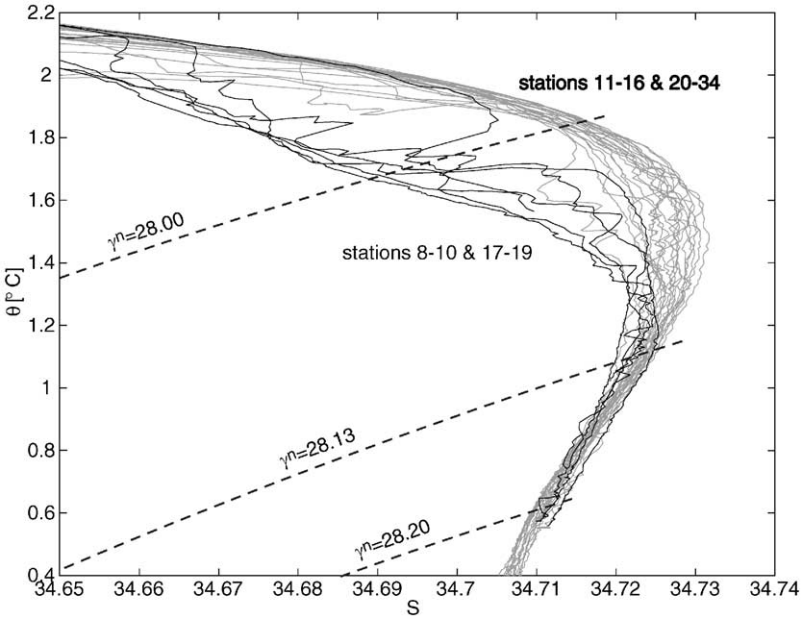

Fig. 8. Potential temperature–salinity plot of CDW north of the SACCF in Drake Passage. Curves including the dominant CDW type (see Section 4.4.1) are shown in grey, whereas stations with the less widespread, low-oxygen CDW type are depicted in black. Dashed lines mark selected neutral density contours.

Fig. 8b). Note the very high silicate values in the WSDW fraction with $\gamma^n > 28.29$, which probably arise from dissolution of siliceous sediments as the water mass spreads along the ocean floor.

The outlined spatial distribution of the two WSDW types highlights their likely different fates. WSDW from the South Sandwich Trench occupies the region just south of the Falkland Ridge and can thus spill into the Argentine Basin to feed the deep western boundary current (Whitworth et al., 1991). In contrast, the Scotia Sea variety constitutes the bulk of the WSDW spreading westward into the Malvinas Chasm (Cunningham and Barker, 1996) and may upwell there into the CDW layer, thereby following a more diffuse path out of the basin. Recirculation of this WSDW component following the retroflection of the SACCF is also possible [Arhan et al. (1999, their Fig. 12)], as cyclonic flow relative to the bottom is suggested by the doming of deep isopycnals in the western Georgia Basin. Some leakage of the Scotia Sea variety into the Argentine Basin along this route cannot be ruled out with the available data.

4.2. Circumpolar Deep Water

4.2.1. The inflow through Drake Passage

CDW is observed (Fig. 3) entering the Scotia Sea through Drake Passage between the SAF at 57°S (where it is found between 800 m and the ocean floor) and the SB at 62.5°S (where UCDW intrudes into the mixed layer). CDW characteristics in Drake Passage show a previously unreported bimodal distribution. In the more widespread mode (grey curves in Fig. 8) θ–S curves align close to the outer rim of the envelope of curves; in the other (black curves in Fig. 8), CDW in the $\gamma^n < 28.13$ density class is cooler (by 0.2°C), fresher (by 0.02), poorer in oxygen (by 15 μmol kg^{-1}) and richer in silicate (by 15 μmol kg^{-1}) along isopycnals. The latter CDW type is found at the SAF and north of the PF in the depression of isopycnals near 59°S (stations 17–19). Its presence at these locations is denoted most clearly by two lenses with oxygen values below 160 μmol kg^{-1} (Fig. 3c) and local upward protrusions of silicate contours (Fig. 3d).

Tsuchiya and Talley (1998) observed a water mass with characteristics similar to those of the low-oxygen CDW type flowing south off southern Chile at 54°S. They also showed (Fig. 4) that the shallowest isopycnal that is constrained to lie within the Southeast Pacific Basin is close to $\sigma_4 = 45.90$. Thus, only less dense waters can mix isopycnically with those of the subtropical Pacific. In Drake Passage, that isopycnal is equivalent to $\gamma^n = 28.13$, which marks the location in θ–S space at which the curves of the two CDW modes start diverging (Fig. 8). It is conceivable that some CDW from the northern ACC may undergo a northward excursion upon reaching the Southeast Pacific Basin, interact with deep waters of the subtropical Pacific and return south along the South American continental slope with modified properties. Reid (1997) deduced a deep cyclonic circulation pattern in the Southeast Pacific Basin that would support the proposed flow. Particularly enlightening is his map of oxygen on $\sigma_2 = 36.88$ ($\gamma^n \simeq 27.90$) in the Pacific Ocean (Reid, 1997, Fig. 12c), where a set of low oxygen contours follow the deep cyclonic flow in the Southeast Pacific Basin from the subtropics to the southern tip of South America and thus insinuate a link to the low oxygen lens in northern Drake Passage. The presence of the low-oxygen CDW type at 59°S is likely due to the shedding of an anticyclonic eddy from the SAF, as is suggested by the reversal in the slope of the isopycnals there. Southward export of northern waters across the SAF through episodic events is common in the northwestern Scotia Sea (Peterson and Whitworth, 1989).

South of the PF, the potential temperature and salinity of UCDW lighter than $\gamma^n = 27.88$ (the density at the core of the oxygen minimum) are decreased by mixing with Antarctic Surface Water. As a result a potential temperature maximum is induced (Fig. 3a), and oxygen values are increased (Fig. 3c), above the oxygen minimum (Sievers and Nowlin, 1984). The potential temperature maximum and the oxygen minimum are absent in the eddy-like feature at 62.5°S, and terminate at the SB (Orsi et al., 1995). Vestiges of both these signatures are, however, observed penetrating the Bransfield Strait. The disappearance of UCDW south of the SB is accompanied by a change in character of LCDW, which is exposed to colder, fresher waters off the western Antarctic Peninsula. The LCDW found below the $\gamma^n = 28.20$ isopycnal between the PF and the SB is SPDW, as denoted by the extremely high near-bottom silicate values of approximately 140 μmol kg^{-1} (Sievers and Nowlin, 1984). North of the SACCF, SPDW flows adjacent to the sea floor, whereas south of the front it overlies WSDW. A sharp distinction between the thermohaline properties of the densest SPDW north and south of the SACCF (Fig. 5) indicates the onset of diapycnal mixing with WSDW in Drake Passage.

4.2.2. *WDW in the Weddell–Scotia Confluence*

WDW is observed along the South Scotia Ridge in the depth range 200–1500 m (Fig. 3) as far west as the Antarctic Slope Front (Whitworth et al., 1998) at 50.2°W. West of the front, a mixture of cold ($\theta < -0.2$°C), fresh ($S < 34.60$), oxygenated (> 230 μmol kg^{-1}), silicate-poor (< 110 μmol kg^{-1}) waters with a high proportion of low salinity shelf water from the northwestern Weddell Sea dominates the hydrography [Whitworth et al. (1994) grouped these waters under the term 'Bransfield Strait waters']. The properties of WDW west of the South Orkney Islands are highly variable due to interaction with Bransfield Strait waters (Fig. 3). WDW with characteristics similar to those west of the South Orkney Islands is detected in the 1350-m gap near 43°W, overlying the 'ventilated' WSDW overflow observed at the same location (Section 4.1.1).

Within and east of the Orkney Passage, WDW is warmer, more saline, less oxygenated and richer in silicate than further west (Fig. 4). Two distinct WDW types occur in this eastern regime. One has a more pronounced θ/S maximum ($\theta > 0.55$°C, $S > 34.685$), above which the θ–S relationship slopes linearly towards the characteristics of Antarctic Surface Water (Fig. 4, shaded in grey). This WDW type is observed on the western flanks of the Orkney Passage (stations 74–77) and the Bruce Passage (stations 85–86). Reference to Whitworth et al. (1994) reveals that its thermohaline properties are typical of the Weddell Gyre and thus suggests that at those sites WDW is being injected into the Weddell–Scotia Confluence from

the south. The second WDW type shows an influence of shelf waters and CDW from the ACC. Like the WDW west of the Orkney Passage, it is marked by a relatively fresh, oxygenated and silicate-impoverished salinity maximum (unshaded small dots in Fig. 4) which it acquires from its shelf water component. At lower densities, however, potential temperature and silicate are increased (and oxygen content is reduced) relative to the first WDW type as a result of interleaving of CDW from the north. Whitworth et al. (1994) referred to this WDW type as 'ACC/Weddell–Scotia Confluence waters'. Owing to their sparse station data lying west of 45°W (Whitworth et al., 1994, Fig. 3), they only reported its presence along a narrow band following the SB. Here, we show that east of the South Orkney Islands to 31°W 'ACC/Weddell–Scotia Confluence waters' are by far the most widespread water mass within the Confluence.

This statement finds support in the southern end of the WOCE A23 repeat section, which encompasses most of the latitudinal range of the Weddell–Scotia Confluence (located between 59°S and 60.5°S in the original WOCE A23 section). The WDW spreading eastwards in this region has 'ACC/Weddell–Scotia Confluence' characteristics (not shown) and so does that within the doming of property contours near 57.5°S (Fig. 3), associated with a cyclonic eddy or meander of the SB. No WDW of the Weddell Gyre type is detected, suggesting that the inflow of WDW into the Confluence along the western flanks of the Orkney Passage and the Bruce Passage is rapidly modified by waters with a shelf water or a CDW component.

4.2.3. CDW in the eastern Scotia Sea

In the WOCE A23 repeat section, CDW of the ACC is observed escaping the Scotia Sea between the SB and South Georgia. Its properties vary dramatically along the section (Fig. 2b) in response to the intensity of mixing with Weddell Sea waters decreasing with distance from the Weddell–Scotia Confluence. Thus, potential temperature and salinity generally increase, and oxygen decreases, northwards along isopycnals. North of the SACCF, a lens with salinity greater than 34.71 is detected in the salinity maximum of LCDW (Fig. 3b) which suggests that the SACCF inhibits mixing with waters of Weddell Sea origin (in Drake Passage and the WOCE A23 repeat section, WSDW is only found south of the SACCF). As a consequence of mixing with Weddell Sea waters, LCDW in the WOCE A23 repeat section is about 0.15°C colder and 0.015 fresher along isopycnals than LCDW between the SACCF and the SB in Drake Passage.

Below the $\gamma^n = 28.20$ isopycnal, the modification affecting the LCDW layer manifests itself as a replacement of the SPDW properties found in Drake Passage by those of WDW in the Weddell–Scotia Confluence. Only at station 118, on the northern flank of the SACCF, may a remnant of the SPDW characteristics be observed near the bottom ($\sim$2500 m). (Although the remnant does not encompass the entire density range of SPDW, we suspect that this may be a consequence of the station spacing not fully resolving a narrow current core.) Potential temperature and salinity within the remnant are elevated with respect to stations further south (Fig. 9). Silicate values, though lower by about 10 μmol kg^{-1} than in Drake Passage, reach a maximum of 125 μmol kg^{-1} at the bottom (Fig. 3d), which compares well with the SPDW silicate content observed by Peterson and Whitworth (1989) downstream of the Scotia Sea in the Falkland Escarpment. Although we do not suggest a link between the two sites (see Section 4.2.4), the existence of a previously unreported route for modified SPDW to escape the Scotia Sea following the SACCF through Georgia Passage is indicated by our data. Further evidence for this route can be gathered from the distribution of the chlorofluorocarbon CFC-11 measured during the WOCE A23 section (Meredith et al. (2001), their Fig. 2d)): at the position of station 118, the concentration is lower than anywhere else in the eastern Scotia Sea on the same isopycnal.

4.2.4. The entry to the western Georgia Basin

CDW in the Scotia Sea can reach the western Georgia Basin by either flowing over the North Scotia Ridge or circumnavigating South Georgia. This leads to a sharp distinction between the CDW found near the PF, which has overflowed the

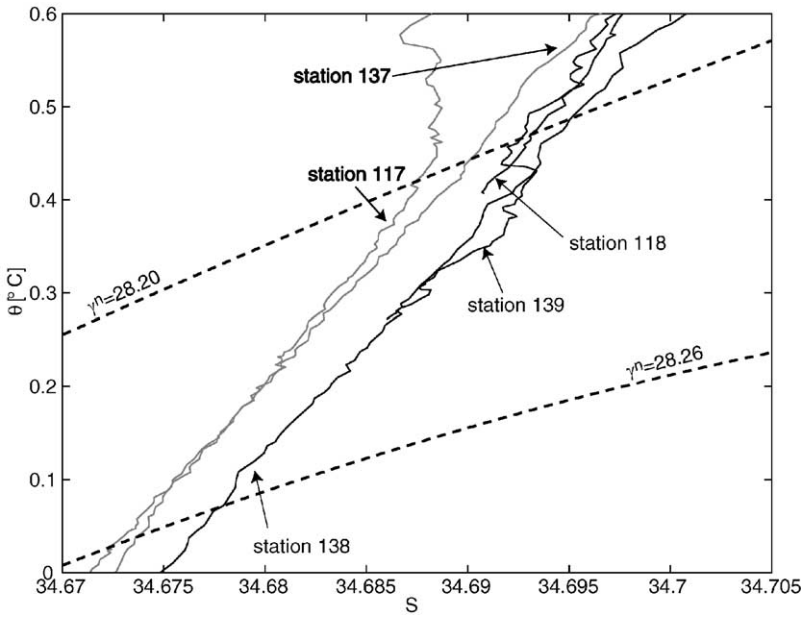

Fig. 9. Potential temperature–salinity plot showing the SPDW remnants outflowing the Scotia Sea. The SPDW outflow south of South Georgia is represented by station 118 and the θ–S characteristics of surrounding waters by station 117. Similarly, stations 138–139 correspond to the SPDW outflow south of the Maurice Ewing Bank, with station 137 exemplifying the thermohaline properties of adjacent waters to the south. Dashed lines are selected neutral density contours.

North Scotia Ridge, and that south of 51.5°S, which has followed the SACCF through the Georgia Passage and is colder (by 0.08°C) and fresher (by 0.007) along isopycnals (Fig. 10). In the region of transition between the two regimes (stations 137–138), CDW shares the PF characteristics above the $\gamma^n = 28.06$ surface only. Between this isopycnal and $\gamma^n = 28.13$ there is interleaving of the two CDW types, whereas for greater densities CDW is identical to that further south. In Drake Passage, the $\gamma^n = 28.06$ isopycnal shoals southwards to 1500 m in the region between the PF and the SACCF (Fig. 3e), a depth that is approximately coincident with that of the bank near 46°W flanking Shag Rocks Passage to the east (Fig. 1). If CDW found at the PF in the western Georgia Basin flowed through the region of Shag Rocks Passage (as is suggested by the trajectory of the PF in Fig. 1), then CDW on the poleward side of the front must have spilled over this bank and densities in excess of $\gamma^n = 28.06$ must have been blocked. It follows that the interleaving observed in the CDW of the western Georgia Basin may have been induced by CDW overflowing the North Scotia Ridge at different locations. Thus, the $\gamma^n = 28.13$ surface marking the densest interleaving ascends to 2000 m between the PF and the SACCF in Drake Passage (Fig. 3e), a depth that is remarkably close to the sill depth of the North Scotia Ridge near 45°W. This suggests that there is little northward transport of CDW over the shallower sector of the North Scotia Ridge east of that longitude.

The restriction on the flow of CDW into the Georgia Basin exerted by the North Scotia Ridge is particularly strong in the SPDW density class. The sector of the ridge southeast of the PF (the hydrographic region to which SPDW is confined in Drake Passage) is shallower than 2000 m everywhere except near Shag Rocks Passage, where it reaches 3200 m (Fig. 1). In comparison, the depth of the $\gamma^n = 28.20$ isopycnal in Drake Passage decreases from 3500 m at the PF to 2500 m at the SACCF (Fig. 3) (these two fronts encompass the hydrographic zone overflowing that sector of the ridge). This suggests the possibility that SPDW

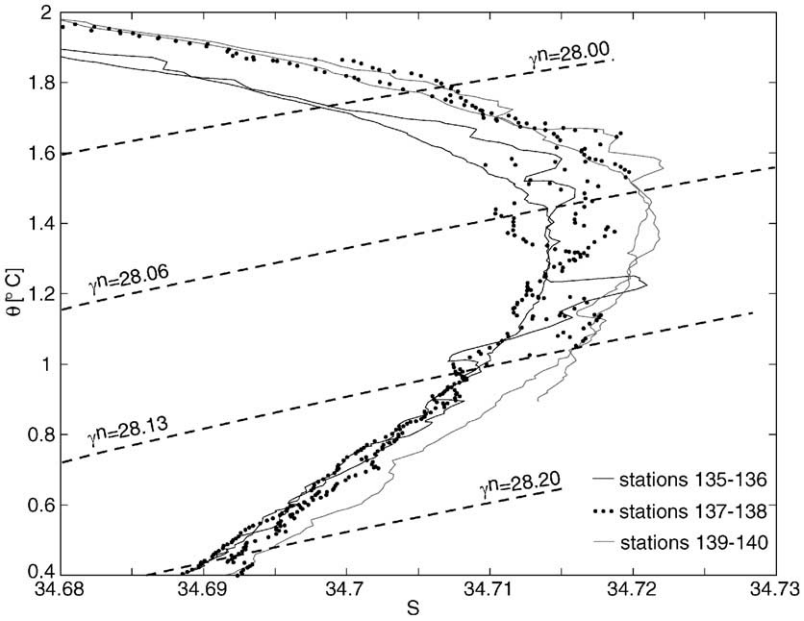

Fig. 10. Potential temperature–salinity plot of LCDW south of the Maurice Ewing Bank. Dashed lines are selected neutral density contours. Stations 135–136 (solid grey lines) illustrate the properties of LCDW advected into the western Georgia Basin through the Northeast Georgia Passage, whereas 139–140 (solid black lines) represent LCDW that has flowed through Shag Rocks Passage with the PF. Stations 137–138 (dotted lines) contain LCDW of the former type at $\gamma^n > 28.13$ and of the latter type at $\gamma^n < 28.06$, with interleaving of the two types at intermediate densities.

can overflow the North Scotia Ridge only at Shag Rocks Passage. As documented by Zenk (1981) from mooring data, leakage of SPDW through Shag Rocks Passage does occur and is intermittent. Arhan et al. (1999) suggested that this leakage might be controlled by mesoscale meanders of the PF. Based on the observation of a SPDW core over the Falkland Escarpment at 41°W and 55°W, they hypothesized a pathway for SPDW around the Maurice Ewing Bank and westward along the escarpment.

Their hypothesis is confirmed by our data. In the western Georgia Basin, we observe a water mass in the neutral density range of SPDW that is warmer and more saline than CDW in the same density class at stations to the south (Fig. 9). Its depth (~3200 m) and location beneath the PF suggest that it has followed the front through Shag Rocks Passage. The SPDW core in the western Georgia Basin has thermohaline properties and silicate content identical to those of the SPDW remnant south of South Georgia.

4.2.5. *The Falkland Plateau overflow*

CDW in the region of the PF in the western Georgia Basin is generally colder (by about 0.07°C) and fresher (by approximately 0.008) along isopycnals than CDW at the PF in Drake Passage. However, at one station above the eastern rim of the Maurice Ewing Bank (station 141) the potential temperature and salinity of CDW are raised substantially, and the salinity maximum of LCDW reaches Drake Passage values. Consideration of the salinity distribution on the transect along the Falkland Plateau (Fig. 3b) suggests that this feature originates from a southward intrusion over the plateau of CDW that has entrained NADW. Contamination of CDW by NADW is in fact detected between 47°W and 49°W, in the region of eastward shallowing of the Falkland Plateau between the sill of the plateau and the western edge of the Maurice Ewing Bank. The confinement of NADW contamination to this region is concordant with a topographically driven southward flow there below the depth of the bank,

followed by an anticyclonic circulation along the southern flank of the bank toward the western Georgia Basin.

As a result of contamination by NADW, the salinity of LCDW west of the Maurice Ewing Bank exceeds 34.73 frequently and attains a peak of 34.74 at 47°W. Entrainment of NADW is observed up to a maximum density of $\gamma^n = 28.11$, which is coincident with the lower boundary of NADW north of the Falkland Plateau [$\sigma_4 = 45.89$, Arhan et al. (1999)]. Below this isopycnal, LCDW has properties that match those of LCDW in the same density class at the PF in the western Georgia Basin (this is reflected in Figs. 3a and b in a bulging of the body of water with $\theta < 1.0$°C and $S < 34.71$ near 2600 m between 46°W and 48°W), suggesting that the fraction of LCDW with density greater than $\gamma^n = 28.11$ has circulated anticyclonically around the northern edge of the Maurice Ewing Bank with little modification.

Fig. 3 shows that the $\gamma^n = 28.00$ isopycnal (the boundary between UCDW and LCDW) is close to the sea floor of the Maurice Ewing Bank, indicating that, unlike in the case of LCDW, the UCDW circulation may not be tied to topography. The θ–S properties of UCDW in the region are consistent with this idea. Three UCDW types are apparent in the region (Fig. 11a) with properties characteristic of the poleward side of the PF (the Antarctic Zone), its equatorward side (the Polar Frontal Zone) or a zone of transition associated with the front itself. All stations above the Maurice Ewing Bank except one sampled UCDW with PF characteristics (at station 146, UCDW had Antarctic Zone characteristics), whereas UCDW has Polar Frontal Zone properties to the west of the bank and Antarctic Zone properties in much of the western Georgia Basin (Fig. 11b). This distribution is suggestive of a cyclonic circulation of UCDW over the bank, possibly associated with a retroflection of the upper layers of the PF (following a topographically induced decoupling from the lower layers), or an eddy shed by the front. (Note that the large apparent width of the PF over the bank is probably caused by its near-zonal alignment there.) In a map of annual mean sea surface temperature, Moore et al. (1997, their Plate 1) observe a bulge of relatively cold water at the position of the Maurice Ewing Bank that may be the signature of a stationary meander of the PF there. The detection of UCDW with Polar Frontal Zone characteristics between the sill of the Falkland Plateau and the Maurice Ewing Bank suggests that UCDW in the region is advected northward over the plateau, which would imply a local reversal of the flow direction near the boundary with LCDW.

West of the sill, CDW overflows the Falkland Plateau between 49°W and 55°W (Fig. 3). Detailed inspection of the properties of CDW in this longitude range is indicative of two distinct pathways for CDW to spill northward over the plateau. One of the pathways crosses the region of the Falkland Plateau in the vicinity of 49.5°W. It contains CDW that has flowed through Shag Rocks Passage on the northern flank of the PF, apparently implying a topographically induced lateral splitting of the front at the southern flank of the plateau. Accordingly, the local thermohaline characteristics of LCDW show vestiges of those near the PF in Drake Passage while agreeing closely with LCDW properties at the PF in the western Georgia Basin (Fig. 12). A presence of the low-oxygen CDW type found north of the PF in Drake Passage (Fig. 8) is also revealed by the decreased salinity and oxygen content of UCDW at 49.5°W in relation to surrounding stations. These can be observed in Fig. 3b as a divergence of the 34.71 isohaline and the $\gamma^n = 28.0$ isopycnal near 2000 m, and in Fig. 3c as a convergence of the 170 μmol kg^{-1} contour and the $\gamma^n = 28.0$ isopycnal near the same depth. Although indicative of northward flow relative to the bottom, this CDW contains little geostrophic vertical shear and a significant barotropic component [such as observed in other topographically controlled jets e.g., Gordon et al. (2001)] is anticipated.

The second pathway followed by CDW spilling northward over the Falkland Plateau crosses our section near 53°W and is associated with the SAF. Similarly to the first pathway, the low salinity and low oxygen signals of the anomalous CDW type found at the SAF in Drake Passage are detectable at 53°W. Even in the proximity of the SAF, CDW

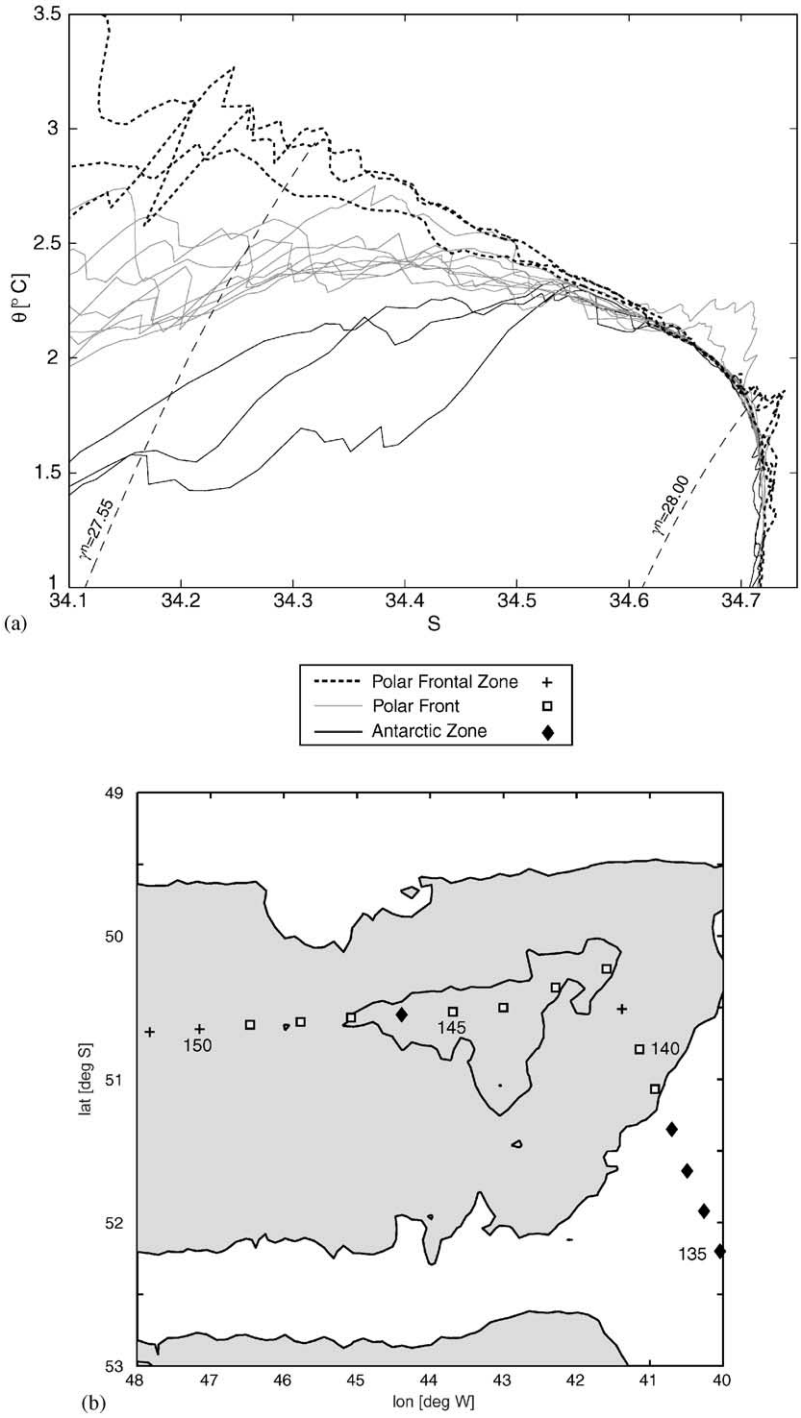

Fig. 11. (a) Potential temperature–salinity plot of UCDW in the vicinity of the Maurice Ewing Bank. Dashed lines are the isopycnic bounds of UCDW. Curves are plotted differently for the three hydrographic regions of the Polar Frontal Zone (dotted), the PF (solid grey) and the Antarctic Zone (solid black). (b) Geographical distribution of UCDW in each hydrographic region. Stations with Polar Frontal Zone UCDW are marked by crosses, whereas those with PF and Antarctic Zone UCDW are indicated by squares and diamonds, respectively. Isobaths are 1500 and 3000 m from Smith and Sandwell (1997).

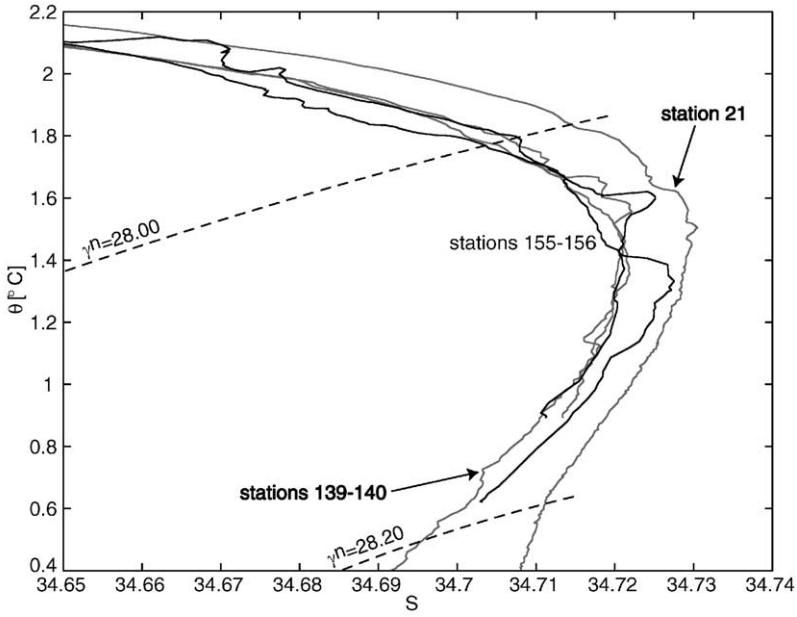

Fig. 12. Potential temperature–salinity plot to illustrate the split of CDW near the PF in the Malvinas Chasm. Station 21 exemplifies the properties of CDW at the PF in Drake Passage. Stations 139–140 are located at the PF in the western Georgia Basin. Stations 155–156 above the Falkland Plateau share their basic θ–S characteristics with stations 139–140, but contain remnants of relatively unmixed CDW from Drake Passage. Dashed lines are selected neutral density contours.

has been weakly cooled (by about 0.03°C) and freshened (by approximately 0.004) in its transit through the Scotia Sea. The bulk of the volume of CDW advected along this pathway is in the UCDW density range, though a core of LCDW is sampled at a depth of 2000 m at 52°W on the southern flank of the SAF (Fig. 3). The depth and longitude of this core are close to those of a passage in the North Scotia Ridge at 54.5°W just to the east of Burdwood Bank (Fig. 1) through which the climatological trajectory of the SAF (and, presumably, much of the LCDW contained in the core) passes.

Separating the two pathways described above, a dome of isopycnals centred at 50.5°W is observed. There, an isolated lens of UCDW with properties typical of the PF is encountered that suggests the presence of a cyclonic eddy, probably shed from the southern side of the Falkland Plateau. Our detection of LCDW overflowing the plateau northward along two distinct routes corroborates the conjecture of Arhan et al. (1999), who invoked the existence of two overflow sites to account for the double core of LCDW present in the deep boundary current at the Falkland Escarpment near 55°W.

5. Summary and conclusions

The descriptions in Section 4 provide the basis for a schematic synthesis of the modification and pathways of the deep water masses of the Scotia Sea (Fig. 13).

WSDW enters the Scotia Sea principally by overflowing the South Scotia Ridge. A relatively cold and fresh variety, recently ventilated in the northern Antarctic Peninsula, spills over the ridge west of the Orkney Passage and spreads westward along the deep continental slope of the South Shetland Island Arc to Drake Passage (Fig. 13, pathway 1). More saline WSDW flowing through the Orkney Passage can also reach Drake Passage between the SACCF and the SB through abyssal breaches in the topography of the southern Scotia Sea (pathway 2). WSDW flowing along pathways

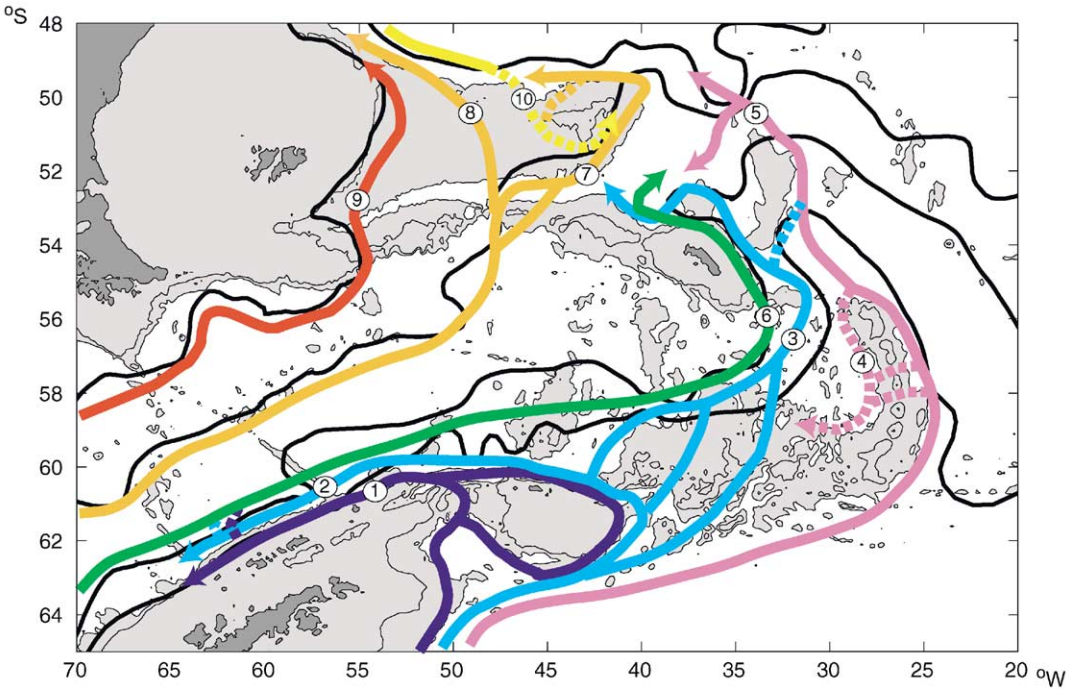

Fig. 13. Schematic pathways of the deep water masses of the Scotia Sea, coloured subjectively to reflect variability in the properties of water masses. The main pathways are numbered for reference in Section 5. Broken segments indicate sporadic or unconfirmed pathways. The bathymetry and frontal patterns have been taken from Fig. 1.

1 and 2 upwells into eastward-flowing CDW without reaching the Pacific Ocean (Orsi et al., 1999).

The bulk of the WSDW overflowing the South Scotia Ridge through and east of the Orkney Passage, however, escapes the Scotia Sea eastwards through the Georgia Passage (pathway 3). Only the $\gamma^n < 28.31$ density class can flow through the passage. A fraction with $\gamma^n < 28.29$ then enters the western Georgia Basin via the Northeast Georgia Passage (pathway 3) and spreads into the Malvinas Chasm, with the higher density class joining higher-salinity WSDW flowing north from the South Sandwich Trench (pathway 5). After circumnavigating the Northeast Georgia Rise, the latter WSDW component can leak into the Argentine Basin or enter the western Georgia Basin, possibly underriding the fresher WSDW from the eastern Scotia Sea. The high salinity WSDW from the South Sandwich Trench may also leak into the eastern Scotia Sea through the Georgia Passage or one of the gaps in the South Sandwich Island Arc (pathway 4) and alter the abyssal properties south of the SB.

The properties of the CDW entering the Scotia Sea through Drake Passage display a previously undetected bimodal distribution. The more widespread mode corresponds to CDW transported by the ACC from the west. The other is found mainly at the SAF and may be associated with a mid-depth jet flowing southward from the subtropical Pacific along the coast of South America. A conspicuous near-bottom silicate maximum identifies SPDW between the PF and the SB.

In the Scotia Sea, the CDW of the ACC mixes vigorously with WSDW and WDW spilling northward over the South Scotia Ridge. As a result, CDW escaping the sea is markedly cooler, fresher and richer in oxygen than that entering through Drake Passage. The extent of ventilation follows a

zonation that can be related to the water mass pathways and the frontal anatomy of the ACC in the region:

- Between the SB in the southeastern Scotia Sea and the region of the SACCF retroflection in the western Georgia Basin (pathway 6), CDW cools by about 0.15°C and freshens by about 0.015 along isopycnals.
- The PF area southeast of the Maurice Ewing Bank contains CDW that has overflowed the North Scotia Ridge along pathway 7. There, the cooling and freshening are reduced to 0.07°C and 0.008, respectively. This also applies to the CDW core overflowing the Falkland Plateau along pathway 8, which may result from a topographically-induced lateral splitting of the PF. In the proximity of the Maurice Ewing Bank, CDW contaminated with NADW can be injected southward (pathway 10) and increase CDW salinity locally.
- In the region of the SAF over the Falkland Plateau, encompassing waters that have overflowed the North Scotia Ridge along pathway 9, CDW has been cooled by about 0.03°C and freshened by about 0.004 along isopycnals.

The modification undergone by CDW in the Scotia Sea results in an almost total erosion of the properties of SPDW. We have found, however, two routes along which remnants of SPDW can escape the Scotia Sea with a resolvable signature. One, along pathway 6, had never been reported. The other, along pathway 7 and through Shag Rocks Passage, had been hypothesized by Arhan et al. (1999) and is thought to feed the deep boundary current at the Falkland Escarpment.

The cooling and freshening of CDW in the Scotia Sea is a significant component of the thermohaline overturning of the Southern Ocean. This can be shown through a simple order of magnitude calculation. Assuming (i) a volume transport of CDW through Drake Passage of about 100 Sv (Sloyan and Rintoul, 2001), (ii) that the CDW of the ACC leaves the Scotia Sea at exactly the same rate, and (iii) a basin-averaged CDW cooling and freshening close to that observed at the PF, would imply a heat (salt) convergence of the order of 3×10^{13}W (8×10^{5}kg s^{-1}) within the CDW layer of the ACC in the Scotia Sea. The former figure is as much as one third of the oceanic heat divergence estimated by Sloyan and Rintoul (2001) for the entire South Atlantic sector between $\sim 40°$S and $\sim 65°$S, whereas the latter represents a non-negligible (albeit difficult to determine accurately) fraction of the salt flux increase between Drake Passage and south of Africa. (Note that changes in the heat and salt content of the ACC in the Scotia Sea are opposite in sign to those in the entire Atlantic sector due to the influence of NADW east of the Scotia Sea.) Significantly, the CDW modification in the Scotia Sea takes place immediately upstream of the Argentine Basin, where the ACC system exchanges deep waters with the subtropical gyre of the South Atlantic. The signal of this modification is propagated rapidly along the deep western boundary current (which is a crucial component of the meridional heat and salt fluxes of the South Atlantic) and can reach the subtropical gyre with relatively little alteration (Wienders et al., 2000). In a subsequent study, we will combine the ALBATROSS hydrographic data set and inverse techniques to investigate the nature of the water mass modification described in this work and establish the role of the Scotia Sea in the thermohaline overturning of the Southern Ocean.

Acknowledgements

We are grateful to the officers, scientists and crew of RRS *James Clark Ross* for their invaluable assistance in the collection of the ALBATROSS data set. ALBATROSS was funded by the Natural Environment Research Council through grant GR3/11654. We warmly thank M. Arhan, E.L. McDonagh and M.P. Meredith for useful discussions, and A.H. Orsi for providing the digitised frontal positions of Orsi et al. (1995). This study benefited from the comments of three anonymous reviewers, to whom we extend our gratitude.

References

Arhan, M., Heywood, K.J., King, B.A., 1999. The deep waters from the Southern Ocean at the entry to the Argentine Basin. Deep-Sea Research II 46, 475–499.

Callahan, J.E., 1972. The structure and circulation of deep water in the Antarctic. Deep-Sea Research 19, 563–575.

Carmack, E.C., Foster, T.D., 1975. On the flow of water out of the Weddell Sea. Deep-Sea Research 22, 711–724.

Cunningham, A.P., Barker, P.F., 1996. Evidence for westward-flowing Weddell Sea Deep Water in the Falkland Trough, western South Atlantic. Deep-Sea Research I 43, 643–654.

Fahrbach, E., Rohardt, G., Schröder, M., Strass, V., 1994. Transport and structure of the Weddell Gyre. Annales Geophysicae 12, 840–855.

Fahrbach, E., Rohardt, G., Scheele, N., Schröder, M., Strass, V., Wisotzki, A., 1995. Formation and discharge of deep and bottom water in the northwestern Weddell Sea. Journal of Marine Research 53, 515–538.

Gordon, A.L., Visbeck, M., Huber, B., 2001. Export of Weddell Sea Deep and Bottom Water. Journal of Geophysical Research 106, 9005–9017.

Gordon, A., Weiss, R.F., Smethie Jr., W.M., Warner, M.J., 1992. Thermocline and intermediate water communication between the South Atlantic and Indian Oceans. Journal of Geophysical Research 97, 7223–7240.

Heywood, K.J., Stevens, D.P., 2000. ALBATROSS cruise Report. UEA Cruise Report series No. 6. UEA publications, Norwich, UK.

Jackett, D.R., McDougall, T.J., 1997. A neutral density variable for the world's oceans. Journal of Physical Oceanography 27, 237–263.

Locarnini, R.A., Whitworth III, T., Nowlin Jr., W.D., 1993. The importance of the Scotia Sea on the outflow of Weddell Sea Deep Water. Journal of Marine Research 51, 135–153.

Mantyla, A.W., Reid, J.L., 1983. Abyssal characteristics of the world ocean waters. Deep-Sea Research 30, 805–833.

Meredith, M.P., Naveira Garabato, A.C., Stevens, D.P., Heywood, K.J., Sanders, R.J., 2001. Deep and bottom waters in the eastern Scotia Sea: Rapid changes in properties and circulation. Journal of Physical Oceanography 31, 2157–2168.

Moore, J.K., Abbott, M.R., Richman, J.G., 1997. Variability in the location of the Antarctic Polar Front (90°–20°W) from satellite sea surface temperature data. Journal of Geophysical Research 102, 27825–27833.

Nowlin Jr., W.D., Zenk, W., 1988. Currents along the margin of the South Shetland Island Arc. Deep-Sea Research 35, 805–833.

Orsi, A.H., Johnson, G.C., Bullister, J.L., 1999. Circulation, mixing and production of Antarctic Bottom Water. Progress in Oceanography 43, 55–109.

Orsi, A.H., Nowlin Jr., W.D., Whitworth III, T., 1993. On the circulation and stratification of the Weddell Gyre. Deep-Sea Research I 40, 169–203.

Orsi, A.H., Whitworth III, T., Nowlin Jr., W.D., 1995. On the meridional extent and fronts of the Antarctic Circumpolar Current. Deep-Sea Research I 42, 641–673.

Peterson, R.G., Whitworth III, T., 1989. The subantarctic and Polar fronts in relation to deep water masses through the southwestern Atlantic. Journal of Geophysical Research 94, 10817–10838.

Reid, J.L., 1997. On the total geostrophic circulation of the Pacific Ocean: flow patterns, tracers and transports. Progress in Oceanography 39, 263–352.

Reid, J.L., Nowlin Jr., W.D., Patzert, W.C., 1977. On the characteristics and circulation of the southwestern Atlantic Ocean. Journal of Physical Oceanography 7, 62–91.

Rintoul, S.R., 1991. South Atlantic interbasin exchange. Journal of Geophysical Research 97, 5493–5550.

Sievers, H.A., Nowlin Jr., W.D., 1984. The stratification and water masses at Drake Passage. Journal of Geophysical Research 89, 10489–10514.

Sloyan, B.M., Rintoul, S.R., 2001. The Southern Ocean limb of the global deep overturning circulation. Journal of Physical Oceanography 31, 143–173.

Smith, W.H.F., Sandwell, D.T., 1997. Global sea floor topography from satellite altimetry and ship depth soundings. Science 277, 1956–1962.

Stommel, H.M., Arons, A.B., 1960a. On the abyssal circulation of the world ocean. I. Stationary planetary flow patterns on a sphere. Deep-Sea Research 6, 140–154.

Stommel, H.M., Arons, A.B., 1960b. On the abyssal circulation of the world ocean. II. An idealized model of the circulation pattern and amplitude in oceanic basins. Deep-Sea Research 6, 217–233.

Trathan, P.N., Brandon, M.A., Murphy, E.J., Thorpe, S.E., 2000. Transport and structure within the Antarctic Circumpolar Current to the north of South Georgia. Geophysical Research Letters 27, 1727–1730.

Tsuchiya, M., Talley, L.D., 1998. A Pacific hydrographic section at 88°W. Water–property distribution. Journal of Geophysical Research 103, 12899–12918.

Warren, B.A., 1981. Deep circulation of the world ocean. Evolution of physical oceanography. In: B.A. Warren, C. Wunsch (Ed.), MIT Press, Cambridge, MA, pp. 6–41.

Whitworth III, T., Nowlin Jr., W.D., 1987. Water masses and currents of the Southern Ocean at the Greenwich Meridian. Journal of Geophysical Research 92, 6462–6476.

Whitworth III, T., Nowlin Jr., W.D., Pillsbury, R.D., Moore, M.I., Weiss, R.F., 1991. Observations of the Antarctic circumpolar current and deep boundary current in the southwest Atlantic. Journal of Geophysical Research 96, 15105–15118.

Whitworth III, T., Nowlin Jr., W.D., Orsi, A.H., Locarnini, R.A., Smith, S.G., 1994. Weddell Sea Shelf Water in the Bransfield Strait and Weddell–Scotia Confluence. Deep-Sea Research I 41, 629–641.

Whitworth III, T., Orsi, A.H., Kim, S.-J., Nowlin Jr., W.D., 1998. Water masses and mixing near the Antarctic Slope Front. Antarctic Research Series 75, 1–27.

Wienders, N., Arhan, M., Mercier, H., 2000. Circulation at the western boundary of the South and Equatorial Atlantic. Exchanges with the ocean interior. Journal of Marine Research 58, 1007–1039.

Zenk, W., 1981. Detection of overflow events in the Shag Rocks Passage, Scotia Ridge. Science 213, 1113–1114.